Journal of Mathematical Biology (2021) 83:6
https://doi.org/10.1007/s00285-021-01627-w

Mathematical Biology

Signaling gradients in surface dynamics as basis for planarian regeneration

Arnd Scheel[1] · Angela Stevens[2] · Christoph Tenbrock[2]

Received: 13 August 2019 / Revised: 1 June 2021 / Accepted: 13 June 2021

Abstract
Based on experimental data, we introduce and analyze a system of reaction-diffusion equations for the regeneration of planarian flatworms. We model dynamics of head and tail cells expressing positional control genes that translate into localized signals which in turn guide stem cell differentiation. Tissue orientation and positional information are encoded in a long range *wnt*-related signaling gradient. Our system correctly reproduces typical cut and graft experiments, and improves on previous models by preserving polarity in regeneration over orders of magnitude in body size during growth phases. Key to polarity preservation in our model flatworm is the sensitivity of cell differentiation to gradients of *wnt*-related signals relative to the tissue surface. This process is particularly relevant in small tissue layers close to cuts during their healing, and modeled in a robust fashion through dynamic boundary conditions.

1 Introduction

Planarians are nonparasitic flatworms commonly found in freshwater streams and ponds (Reddien and Alvarado 2004; Rink 2018) with a body size in the mm-scale. The best experimental data is available for the species "Schmidtea mediterranea", which is 1–20 mm long and consists of 100.000 to more than 2.000.000 cells. Planarians

✉ Arnd Scheel
scheel@umn.edu

Angela Stevens
angela.stevens@wwu.de

Christoph Tenbrock
christoph.tenbrock@gmail.com

[1] School of Mathematics, University of Minnesota, 206 Church St. S.E.,, Minneapolis, MN 55455, USA

[2] Applied Mathematics, University of Münster (WWU), Einsteinstr. 62, D-48149 Münster, Germany

Published online: 26 June 2021

possess the ability to regenerate after rather severe injuries to their body. When small tissue parts are cut from the flatworm—in extreme cases just 0.5% of the original size—these can regenerate to a fully functioning and intact organism (Reddien and Alvarado 2004) with head and tail positioned such that the original orientation of the tissue fragment is respected. When tissue parts are cut from a donor and grafted into a host, the newly created planarian integrates the old positional information of the tissue fragment from the donor with the new positional information it obtains from the host. A better understanding of these processes has a far reaching potential for regeneration in general.

Here, we present a minimal mathematical model, informed by experimental data, that reproduces this fascinating behavior. To the best of our knowledge, our system of reacting and diffusing species is to date the only model that correctly recovers most of the typical cutting and grafting experiments, and preserves polarity during regeneration, even of small tissue fragments. The proposed mechanisms resolve a conundrum in modeling efforts. Many models of spontaneous formation of finite-size structure in unstructured tissue so far, allude to a Turing type mechanism to select a finite wavelength. Activator-inhibitor systems (Meinhardt 2012), have often been discussed, for instance in the context of regeneration in hydra, which is similarly robust as planarian regeneration. Turing's mechanism however does (intentionally) not scale across several orders of magnitude, nor does it incorporate robust selection of polarity.

1.1 The mathematical model

We focus on the ante-posterior (AP) axis of planarians and consider a one-dimensional domain $x \in [-L, L]$, populated by different cell types and signals. Head cells $\mathbf{h}$ and tail cells $\mathbf{d}$ generate corresponding signals $\mathbf{u_h}$ and $\mathbf{u_d}$, which activate the respective differentiation of stem cells $\mathbf{s}$. A long-range *wnt*-related signal $\mathbf{w}$, in short *wnt*-signal, encodes orientational information through its gradient. It is produced by tail cells in a saturating fashion, and degraded by reactions with head cells:

$$\partial_t s = D_s \partial_{xx} s + \rho_s(s) - p_h u_h s - p_d u_d s, \tag{1.1}$$
$$\partial_t h = D_h \partial_{xx} h + p_h u_h s - \eta_h h, \tag{1.2}$$
$$\partial_t d = D_d \partial_{xx} d + p_d u_d s - \eta_d d, \tag{1.3}$$
$$\partial_t u_h = D_{u_h} \partial_{xx} u_h + h^2(r_0 - r_1 u_h) - r_2 u_h d - r_3 u_h, \tag{1.4}$$
$$\partial_t u_d = D_{u_d} \partial_{xx} u_d + d^2(r_0 - r_1 u_d) - r_2 u_d h - r_3 u_d, \tag{1.5}$$
$$\partial_t w = D_w \partial_{xx} w - p_w h w + p_w d(1 - w). \tag{1.6}$$

Stem cells proliferate with saturating rate and undergo apoptosis (Baguñ et al. 1990), which is encoded in $\rho_s(s) = p_s \frac{s}{1+s} - \eta_s s$. Stem cells also differentiate irreversibly into head and tail cells, guided by positional control genes, which are modeled by the respective related localized signals u_h, u_d. Those signals are produced by head and tail cells up to a saturation level, with rates r_0 and r_1 and decay with rate r_3. This interaction works during both, normal tissue turnover and regeneration (Reddien and

Alvarado 2004). Head and tail cells result from stem cell differentiation and do not proliferate. They undergo apoptosis and degrade the signal associated with the other cell type with rate r_2.

The quadratic dependence of the production of u_h and u_d on h and d corresponds to higher order molecular kinetics, quadratic here in their simplest form. Replacing these reactions by first-order kinetics, linear in h, d, would result in spontaneous growth of head and tail regions caused by a linear instability of the zero state; see (4.1) in our analysis and model reduction in Sect. 4 based on tristability, that is, linear stability of head-only, tail-only, and zero states. The quadratic dependence postulated here suppresses this instability and we suggest that some effective higher-order kinetics are indeed crucial there. We used the same parameter p_w for production and degradation of w, since differing rates showed qualitatively similar outcomes in our simulations. Finally, random motion of cells and diffusion of signal molecules are modeled through the diffusion coefficients D_j.

Writing $U(t,x) = (s,h,d,u_h,u_d,w)(t,x)$, $\mathcal{D} = \operatorname{diag}(D_s, D_h, D_d, D_{u_h}, D_{u_d}, D_w)$ and $\mathcal{F} = (F_s, F_h, F_d, F_{u_h}, F_{u_d}, F_w)$ in the system (1.1)–(1.6), we find

$$\partial_t U = \mathcal{D} U_{xx} + \mathcal{F}(U). \tag{1.7}$$

We prescribe inhomogeneous Dirichlet boundary conditions $U_{x=\pm L} = U_\pm$ and evolution equations for the time dependent Dirichlet data

$$\frac{\mathrm{d}}{\mathrm{d}t} U_\pm = -\frac{1}{\gamma} \mathcal{D}\, \partial_\nu U|_{x=\pm L} + \mathcal{F}(U_\pm) + \mathcal{B}, \tag{1.8}$$

where $\partial_\nu U|_{x=\pm L} = \pm\, \partial_x U(t,x)|_{x=\pm L}$ denotes the normal derivative. We think of $U_\pm$ as concentrations in a boundary compartment of length γ where concentrations are spatially constant. Fluxes $-\frac{1}{\gamma}\mathcal{D}\, \partial_\nu U|_{x=\pm L}$ ensure mass conservation up to kinetics,

$$\begin{aligned}\frac{\mathrm{d}}{\mathrm{d}t}\left(\int U + \sum_\pm \gamma U_\pm\right) &= \int \mathcal{F}(U) + \sum_\pm \left(\mathcal{D}\partial_\nu U|_{\pm L} + \gamma \frac{\mathrm{d}}{\mathrm{d}t} U_\pm\right) \\ &= \int \mathcal{F}(U) + \gamma \sum_\pm \left(\mathcal{F}(U_\pm) + \mathcal{B}\right).\end{aligned}$$

Kinetics here are identical to those in the bulk of the domain up to a new term $\mathcal{B}$, present in the dynamics for $s_\pm$, $h_\pm$, and $d_\pm$, that represents a boundary-specific stem-cell differentiation mechanism through rates $\Psi^\pm_{h/d}$,

$$\frac{\mathrm{d}}{\mathrm{d}t} s_\pm = -\frac{1}{\gamma} D_s\, \partial_\nu s|_{x=\pm L} + F_s - \Psi^\pm_h s - \Psi^\pm_d s\,, \tag{1.9}$$

$$\frac{\mathrm{d}}{\mathrm{d}t} h_\pm = -\frac{1}{\gamma} D_h\, \partial_\nu h|_{x=\pm L} + F_h + \Psi^\pm_h s\,, \tag{1.10}$$

$$\frac{\mathrm{d}}{\mathrm{d}t} d_\pm = -\frac{1}{\gamma} D_d\, \partial_\nu d|_{x=\pm L} + F_d + \Psi^\pm_d s\,. \tag{1.11}$$

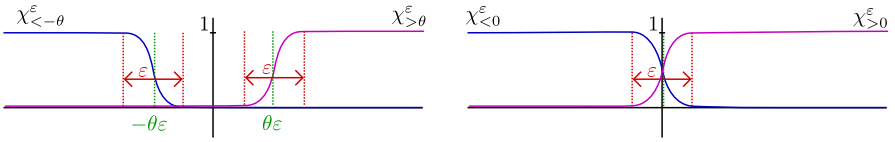

Fig. 1 Schematic plot of the smoothed indicator functions χ^ε that detect positive and negative values of the gradient, respectively, with offset θ and sensing thresholds ε

The differentiation is triggered by lack of head or tail cells, and directed according to the sign of $\partial_v w$, explicitly through $\Psi^\pm_{h/d} = \Psi_{h/d}(h, d, \partial_v w)|_{x=\pm L}$,

$$\Psi_h = \tau(1-h)(1-d)\chi^\varepsilon_{>\theta}(\partial_v w), \quad \text{and} \quad \Psi_d = \tau(1-h)(1-d)\chi^\varepsilon_{<-\theta}(\partial_v w).$$

Here $\tau \gg 1$ is the rate of differentiation, and the χ^ε are smoothed versions of the characteristic function, for example

$$\begin{aligned} \chi^\varepsilon_{>\theta}(\xi) &= \frac{1}{2}\Big[\tanh((\xi - \varepsilon\theta)/\varepsilon) + 1\Big], \\ \chi^\varepsilon_{<-\theta}(\xi) &= \frac{1}{2}\Big[\tanh(-(\xi + \varepsilon\theta)/\varepsilon) + 1\Big]; \end{aligned} \tag{1.12}$$

see Fig. 1 for an illustration.

The steepness ε^{-1} of the smoothed characteristic function can be interpreted as a sensitivity of differentiation with respect to small gradients. The offset θ measures minimal detectable strength of the gradient at the body or wound edge in ε-units. Overall, the kinetics F_s in (1.1) regulate a near-constant supply of stem-cells. As a result, a healthy planarian consists of a high concentration of h near $x = -L$, a high concentration of d near $x = L$, and a near-constant gradient of w in $x \in (-L, L)$; see Fig. 2.

1.2 Boundary dynamics

Differentiation rates in $\Psi^\pm_{h/d}$ do *not* depend on w itself. In particular, concentration levels of the *wnt*-related (or other long-range) signal w are not converted into positional information that in turn directs the differentiation process. Such a direct conversion of signals is often referred to as a French-flag model [see (Wolpert 1969, 1994) and, for planarians, (Rink 2018)] but intentionally not used here:

(1) Positional information is inherently incapable of explaining preservation of polarity. Since regeneration and polarity are robust with respect to the location of cut out tissue fragments, near head, tail, or from the central body region, absolute levels of w play apparently little role in their regeneration.
(2) Positional information is not necessary in the early stages of regeneration, but seemingly relevant only later when the size of functional regions like head or tail are regulated; see Sect. 6.
(3) There is little evidence thus far on the nature of robust biological mechanisms that would translate *wnt*-signal levels into differentiation of stem cells. Postulating

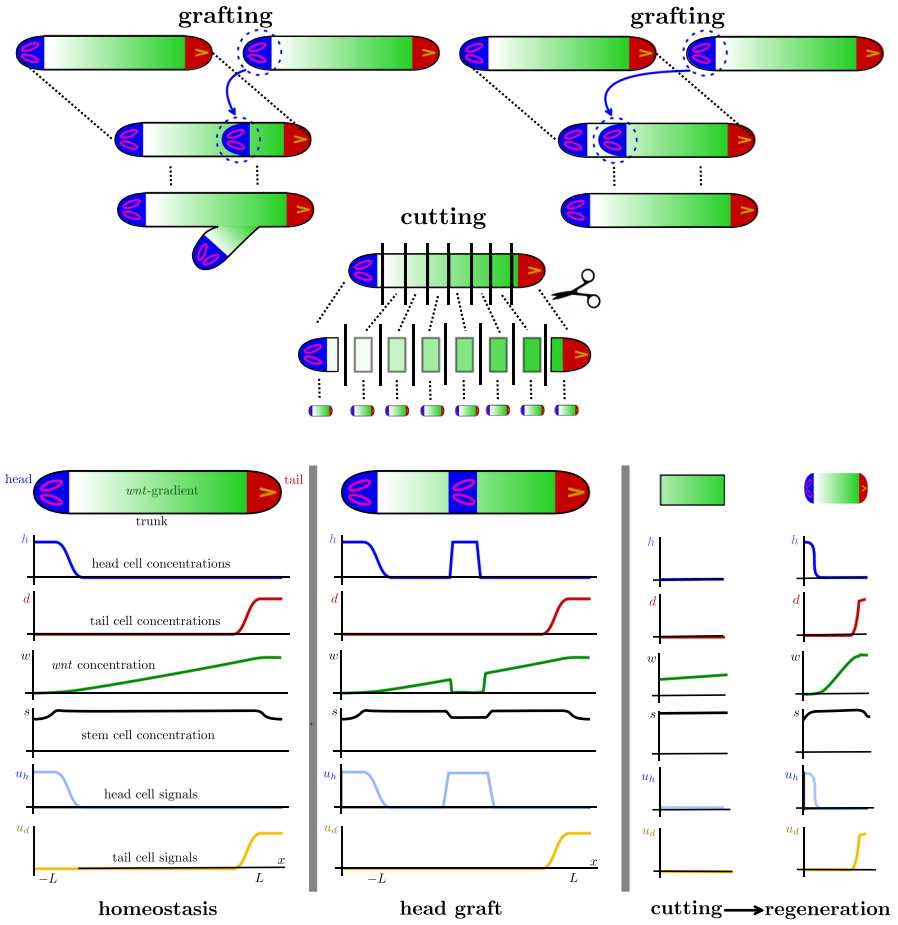

Fig. 2 Typical experiments and their representations in terms of our mathematical model. *Top left:* Schematic illustration of head grafting and regeneration of a two-headed planarian. Top right: Head grafting and regeneration into a normal planarian with one head and tail. *Middle row:* Cutting experiment and regeneration of eight planarians. *Bottom row:* Schematic illustration of experiments on planarians and associated spatial distribution of concentrations h, d, w, s, u_h, u_d. *Homeostasis (left)* has head cells concentrated on the left, tail cells concentrated on the right, a *wnt*-gradient directed towards *wnt*-production in the tail, roughly constant stem cell population with a slight decrease where differentiation into head and tail cells occurs. Head and tail signals are closely mimicking the distribution of head and tail cells. *Grafting (center):* The head region of a donor is grafted into a host, retaining roughly the distribution of cell concentrations and signaling molecules from its original location. *Cutting (right):* A thin fragment (here from the trunk region) retains a small *wnt*-gradient but no head or tail cells. Regeneration in this context refers to reestablishing head and tail cell populations while preserving polarity

such mechanisms would simplify the task of reproducing observed phenomena at the (unnecessary) expense of adding a somewhat poorly substantiated regulatory mechanism.

Cutting experiments eliminate head and/or tail cells, thus influence the *wnt*-pathway and destroy the associated signaling gradient. The terms $\mathcal{B}$ in (1.8) model the strong

local peak of differentiation of stem cells (Wenemoser and Reddien 2010), at wounds inside a formed blastema, guided by *wnt*-signaling (Adell et al. 2010). This reaction, which is specific to wounds with loss of tissue, is not completely understood (Owlarn and Bartscherer 2016), and occurs in our model in regions at the ends of $[-L, L]$. We crucially rely on the detection of the orientation of the *wnt*-gradient relative to the respective body edge. We view this as an in some sense necessary, minimal information, to guide regeneration while at the same time preserving polarity. Looking at the boundary after cutting in Fig. 2, one readily sees that the sign of $\partial_\nu w$ gives clues as to whether differentiation towards head or tail cells should occur.

One can envision several scenarios that enable stem cell differentiation to be guided by gradients of a chemical signal, for instance through comparing signal strength spatially or temporally; see (Alt 1980; Iijima et al. 2002). We do not attempt to model details of this sensing process in the present paper, but simply include a lumped reaction term for differentiation, that depends sharply on the sign of $\partial_\nu w$.

We shall see that our somewhat non standard dynamic (or Wentzel) boundary conditions cannot be readily replaced by, say, Robin boundary conditions. Formally, one could for instance let rates of boundary dynamics tend to infinity or the mass fraction of the boundary compartment γ tend to zero. In the latter case, assuming at the same time rapid reactions $\mathcal{N}_1$, in

$$\frac{\mathrm{d}}{\mathrm{d}t}U_\pm = -\frac{1}{\gamma}\mathcal{D}\,\partial_\nu U|_{x=\pm L} + \mathcal{N}, \qquad \mathcal{N} = \frac{1}{\gamma}\mathcal{N}_1 + \mathcal{N}_2\,,$$

one finds in the limit the mixed boundary condition $\mathcal{D}\partial_\nu U = \mathcal{N}_1(U)$. In Sect. 4.4, we will see that, in this limit to "instantaneous" boundary conditions, the model does not correctly reproduce the phenomena of regeneration. This mathematical curiosity implies for instance the presence of distinguished body regions relevant in regeneration and may relate to the concept of poles separating head and tail regions from the trunk as discussed in Rink (2018) where it is attributed a key role in regeneration.

In another interpretation of dynamic boundary conditions, we can think of compartments for the main body on a uniform grid $x^{(1)}, \dots, x^{(N)}$, with size $x^{(j+1)} - x^{(j)} \equiv dx$ and associated concentrations $U^{(1)}, \dots, U^{(N)}$ such that individual compartments carry masses $dx\,U^{(j)}$. We now add separate boundary compartments $U^{(0)} = U_-$ and $U^{(N+1)} = U_+$ carrying (larger) masses $\gamma U^{(0)}, \gamma U^{(N+1)}$, independent of dx, and impose no-flux boundary conditions on this inhomogeneous spatial grid. Fixing γ and letting $dx \to 0$ we arrive at our dynamic boundary condition. Letting $\gamma \to dx$, we loose the concept of dynamic boundary conditions and should interpret the additional reaction terms $\mathcal{B}$ as nonlinear fluxes. We are not aware of a systematic analysis of such limits, connecting discretization, nonlinear fluxes, and dynamic boundary conditions.

1.3 Outline of the paper

We review biological experiments that motivate our model in Sect. 2 and describe numerical simulations that mimic planarian regeneration in various scenarios in Sect. 3. In Sect. 4, we present analytical results that reduce dynamics to an order parameter c that lumps concentrations of head and tail cells, coupled to the long-range *wnt*-related

Table 1 Parameter values used in simulations throughout, unless noted otherwise

D_s	1	p_s	200	r_0	18	η_s	100
D_h	10^{-3}	p_h	1	r_1	12	η_h	1
D_d	10^{-3}	p_d	1	r_2	6	η_d	1
D_{u_h}	10^{-2}	p_w	10	r_3	6	τ	0.5
D_{u_d}	10^{-2}	γ	0.3			θ	3
D_w	1	L	10			ε	$2 \cdot 10^{-3}$

A discussion on the biological measurements and non-dimensionalization can be found in Tenbrock (2017)

signals $u_{h/d}$ diffuse slowly, while the long-range *wnt*-related signal w has a diffusion constant of order 1. We work on domains of length 10 and attribute a mass fraction $\gamma = 0.3$ to the boundary. We assume very fast proliferation of stem cells $p_s \gg 1$ and fast signaling dynamics r_j relative to cell differentiation. Cell differentiation $p_{h/d}$, apoptosis $\eta_{h/d}$, and differentiation at the tissue edges during wound healing τ occur on a time scale of order 1. The production rate of *wnt*-related signals p_w is faster in comparison.

3.2 Numerical implementation

We implemented the dynamic boundary conditions as time-dependent Dirichlet conditions. The system was solved with grid spacing $dx = 0.01$ and time stepping $5 \cdot 10^{-4}$ using a semi-implicit Euler method. We found little changes from refining spatio-temporal grids and also used MATLAB'S stiff solver ODE15S for comparison with good agreement.

3.3 Results of the numerical simulations

We obtained equilibrium profiles starting with initial conditions that represent head and tail cells in the boundary compartments at the body edges, a uniform distribution of stem cells throughout the trunk, and a uniform *wnt*-signaling gradient. Solving the initial-value problem for a short time, we found that concentrations approached constants in time. Specifically, we used initial conditions

$$\begin{aligned} &h_0(x) \equiv 0,\ h_{-,0} = 1,\ h_{+,0} = 0, \qquad d_0(x) \equiv 0,\ d_{-,0} = 0,\ d_{+,0} = 1, \\ &s_0(x) \equiv 1,\ s_{-,0} = 1,\ s_{+,0} = 1,\ w_0(x) = \frac{x+L}{2L},\ w_{-,0} = 0,\ w_{+,0} = 1, \end{aligned} \tag{3.1}$$

and let u_h, u_d equal h, d. The results match the schematics in Fig. 2. Figure 3 illustrates the dynamic stationary profiles of healthy planarians of different body size in our mathematical model.

The linear concentration profile in the *wnt*-signal is quite robust under dramatic changes in the domain size. Fixing the width of the boundary compartment γ and varying L we found robust homeostasis between $L = 0.005$ (!) and $L = 40$. For